Supporting Information

Axially assembled photosynthetic reaction center mimics composed of tetrathiafulvalene, aluminum(III) porphyrin and fullerene entities

Prashanth K. Poddutoori,[a] Gary N. Lim,[b] Atula S. D. Sandanayaka,[c] Paul A. Karr,[d] Osamu Ito,[e] Francis D'Souza,*[b] Melanie Pilkington,[a] Art van der Est*[a]*

[a]Department of Chemistry, Brock University, 500 Glenridge Ave., St. Catharines, Ontario, Canada L2S 3A1. Email: ppoddutoori@brocku.ca; avde@brocku.ca.

[b]Department of Chemistry, University of North Texas, 11555 Union Circle, 305070, Denton, TX 76203-5017, USA. E-mail: francis.dsouza@unt.edu.

[c]School of Materials Science, Japan Advanced Institute of Science and Technology, Asahidai, Nomi, 923-1292, Japan.

[d]Department of Physical Sciences and Mathematics, Wayne State College, 111 Main Street, Wayne, Nebraska, 68787, USA.

[e]IMRAM, Tohoku University, Katahira, Sendai, 980-8577 Japan.

Synthesis

General. All chemicals, solvents and chromatographic materials were obtained from Aldrich Chemicals and were used as received. Anhydrous *o*-dichlorobenzene (*o*-DCB) from Aldrich was used for all spectroscopic studies. The supporting electrolyte, tetra-*n*-butylammoniumperchlorate (TBAP), for the electrochemistry studies was obtained from Fluka Chemicals. The preparation of the AlPor-Ph-C_{60} dyad and its reference compounds AlPor-Ph and C_{60}-Ph-COOMe have been previously reported.[1,2] Note that the AlPor-Ph-C_{60} dyad was labeled as AlPor-C_{60} in our previous paper. The ^{1}H NMR data for AlPor-Ph-C_{60} (300 MHz, $CDCl_3$): *δ, ppm* 9.05 (s, 8H), 8.14 (d, 8H, *J* = 6.9 Hz), 7.74 (m, 12H), 6.88 (bs, 2H_b), 5.21 (d, 2H_a, *J* = 8.1 Hz), 4.74 (d, 1H, *J* = 9.6 Hz), 4.45 (s, chiral center, 1H), 4.00 (d, 1H, *J* = 9.6 Hz), 2.39 (s, 3H). Synthesis of pyridine appended tetrathiafulvalene derivatives (TTF-py and TTF-Ph-py) were reported elsewhere.[3]

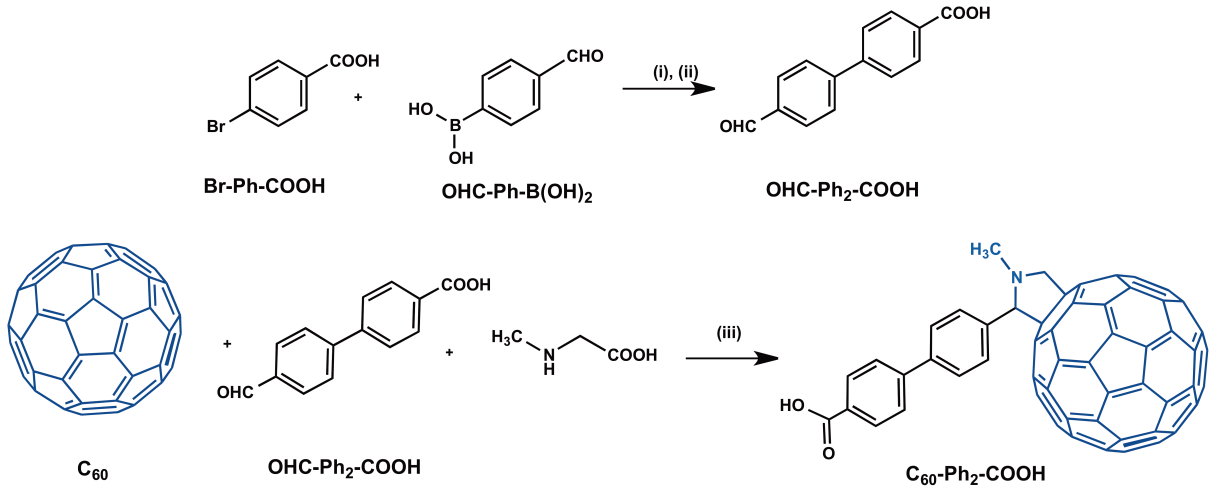

Scheme S1. Synthesis of C_{60}-Ph_2-COOH. Reaction conditions: (i) 2M Na_2CO_3, $Pd(PPh_3)_4$, DMF, stir at 110°C for 12 h under N_2 (ii) 1M HCl and (iii) Toluene, reflux for 5 h under N_2.

Preparation of OHC-Ph$_2$-COOH.[4,5] A mixture of 4-bromobenzoic acid (1.12 g, 5.60 mmol), 4-formylbenzeneboronic acid (1.00 g, 6.70 mmol) and $Pd(PPh_3)_4$ (320 mg, 5 mol%) in DMF (40 mL) was added 2M Na_2CO_3 (8.2 mL, 16.4 mmol). The mixture was heated at 110°C under nitrogen atmosphere. After 12 h the reaction mixture was cooled and the obtained solid was filtered and washed with MeOH (10 mL). Collected filtrate was evaporated to dryness. The residue was added MeOH:H_2O (= 50:10 mL) and acidified with 1M HCl (6 mL). The resulting precipitate was collected, water washed and air-dried. The white solid was washed with chloroform to get the OHC-Ph_2-COOH in a pure form. Yield: 1.20 g (94%). ^{1}H NMR (300 MHz, $(CD_3)_2SO$): *δ, ppm* 13.08 (bs, 1H), 10.10 (s, 1H), 8.07 (d, 2H, *J* =

8.3 Hz), 8.04 (d, 2H, *J* = .8.5 Hz), 7.98 (d, 2H, *J* = 8.3 Hz), 7.91 (d, 2H, *J* = 8.5 Hz). ESI MS: *m/z* 225 $[M-1]^+$ for $C_{14}H_{10}O_3$.

Preparation of C_{60}-Ph_2-COOH. A mixture of C_{60} (100 mg, 0.14 mmol), sarcosine (26 mg, 0.28 mmol) and OHC-Ph_2-COOH (64 mg, 0.28 mmol) in dry toluene (100 mL) was refluxed under nitrogen for 5 h. After reaction time toluene was evaporated and obtained crude product was purified by silica gel column chromatography. The column was eluted with toluene:ethylacetate (= 80:20) and collected the unreacted C_{60} as a first band then desired compound as a second band. The solvent was evaporated to get the pure compound as a brown solid. Yield: 40 mg (30%). ^{1}H NMR (300 MHz, $CDCl_3$): *δ, ppm* 8.15 (d, 2H, *J* = 7.7 Hz), 7.94 (d, 2H, *J* = 7.7 Hz), 7.75 (d, 4H, *J* = 8.2 Hz), 5.06 (d, 1H, *J* = 10.0 Hz), 5.02 (s, 1H), 4.34 (d, 1H, *J* = 10.0 Hz), 2.87 (s, 3H). FAB MS: *m/z* 974 $[M]^+$ for $C_{76}H_{15}NO_2$.

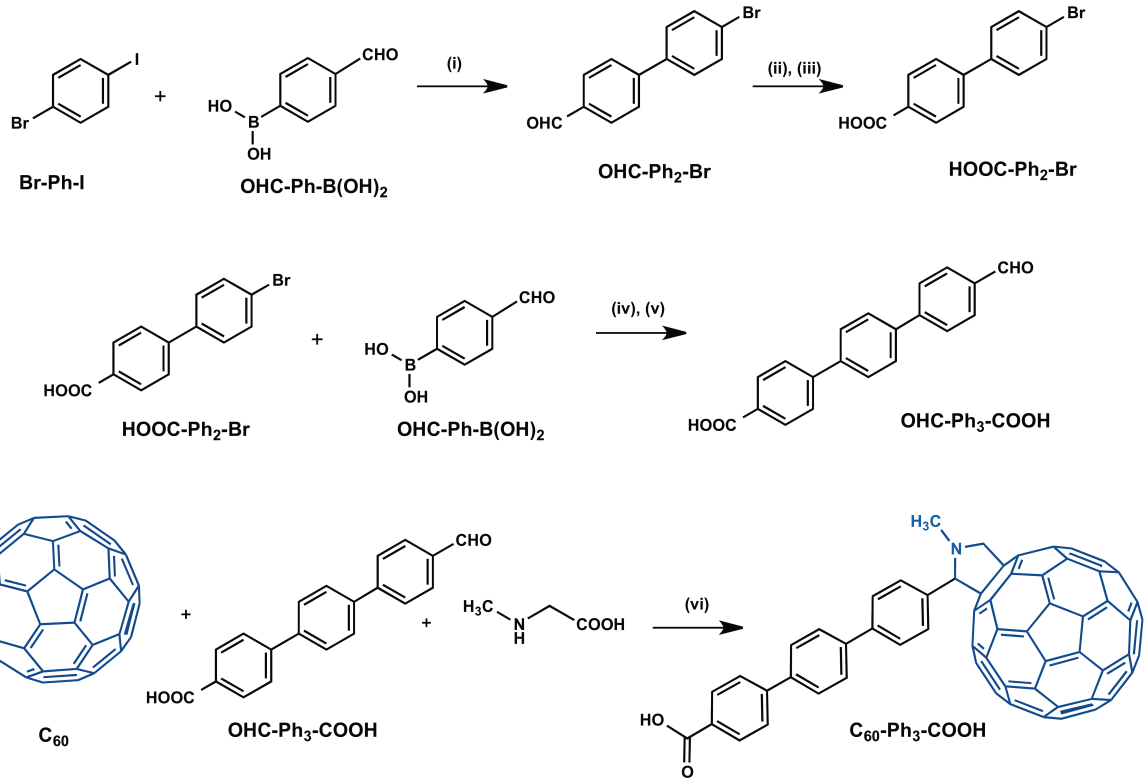

Scheme S2. Synthesis of C_{60}-Ph_3-COOH. Reaction conditions: (i) 2M Na_2CO_3, $Pd(PPh_3)_4$, toluene/ethanol, reflux for 4 h under N_2 (ii) $KMnO_4$, aq. Na_2CO_3, acetone, reflux for 3 h, (iii) Con. HCl, (iv) 2M Na_2CO_3, $Pd(PPh_3)_4$, DMF, stir at 110°C for 5 h under N_2 (v) 1M HCl and (vi) Toluene, reflux for 9 h under N_2.

Preparation of Br-Ph_2-CHO.[6] To a solution of *p*-iodobromobenzene (1.20 g, 4.2 mmol) in toluene (10 mL) was added a catalytic amount of $Pd(PPh_3)_4$ (320 mg, 5 mol%) and aqueous 2M Na_2CO_3 (3 mL, 6

mmol). To this a solution of 4-formylbenzeneboronic acid (1.0 g, 6.6 mmol) in ethanol (10 mL) was added, and the mixture was refluxed for 4 h under nitrogen atmosphere. After cooling, the mixture is extracted three times with dichloromethane and the combined organic phases were washed with water, brine and dried over Na_2SO_4 and the solvent was removed. The residue is purified by silica gel chromatography using dichloromethane:hexane (= 90:10) as eluent, giving the pure compound. Yield: 0.70 g (64%). ^{1}H NMR (300 MHz, $CDCl_3$): *δ, ppm* 10.09 (s, 1H), 7.98 (d, 2H, *J* = 8.7 Hz), 7.74 (d, 2H, *J* = 8.7 Hz), 7.64 (d, 2H, *J* = 8.4 Hz), 7.52 (d, 2H, *J* = 8.4 Hz). FAB MS: *m/z* 261 $[M]^+$ for $C_{13}H_9BrO$.

Preparation of Br-Ph$_2$-COOH.[6] To a solution of Br-Ph$_2$-CHO (350 mg, 1.34 mmol) in 2M Na_2CO_3 (2 mL) and acetone (15 mL) was added aqueous $KMnO_4$ (245 mg in 4 mL of water). The resulting solution was refluxed for 3 h. After cooling, solution was filtered and washed with acetone and water mixture. Collected filtrate was acidified (pH = 4-5) with concentrated hydrochloric acid and obtained precipitate was collected, washed with water and air-dried. The solid was washed with hexane to get the desired compound in a pure form. Yield: 300 mg (80%). ^{1}H NMR (300 MHz, $CDCl_3$): *δ, ppm* 8.18 (d, 2H, *J* = 8.3), 7.68 (d, 2H, *J* = 8.3 Hz), 7.63 (d, 2H, *J* = 8.6 Hz), 7.52 (d, 2H, *J* = 8.6 Hz). FAB MS: *m/z* 277 $[M]^+$ for $C_{13}H_9BrO_2$.

Preparation of OHC-Ph$_3$-COOH. To a suspension of Br-Ph$_2$-COOH (372 mg, 1.34 mmol), OHC-Ph-B(OH)$_2$ (241 mg, 1.60 mmol) and $Pd(PPh_3)_4$ (77 mg, 5 mol%) in DMF (15 mL) was added 2M Na_2CO_3 (2 mL, 4.2 mmol). The mixture was heated at 110 °C for 5 h. After cooling, the solid material was filtered and washed with MeOH (10 mL), and the filtrate was evaporated to dryness. To the residue was added MeOH:H_2O (= 50:10 mL), and the solution was acidified (pH = 4-5) with 1M HCl. The resulting precipitate was collected, washed with water and methanol and air-dried to get the desired compound. Yield: 202 mg (50%). ^{1}H NMR (300 MHz, $CDCl_3$+drops of CD_3OD): *δ, ppm* 10.03 (s, 1H), 8.13 (d, 2H, *J* = 7.4 Hz), 7.97 (d, 2H, *J* = 8.2 Hz), 7.80 (d, 2H, *J* = 7.4 Hz), 7.74 (s, 4H), 7.71 (d, 2H, *J* = 8.2 Hz). EI MS: *m/z* 302 $[M]^+$ for $C_{20}H_{14}O_3$.

Preparation of C$_{60}$-Ph$_3$-COOH. A mixture of C_{60} (78 mg, 0.11 mmol), sarcosine (20 mg, 0.22 mmol) and OHC-Ph$_3$-COOH (66 mg, 0.22 mmol) in dry toluene (100 mL) was refluxed under nitrogen for 9 h. After reaction time toluene was evaporated and obtained crude product was purified by silica gel column chromatography. The column was eluted with toluene:ethylacetate (= 80:20) and collected the unreacted C_{60} as a first band then desired compound as a second band. The solvent was evaporated to

get the pure compound as a brown solid. Yield: 20 mg (17%). ^{1}H NMR (300 MHz, $CDCl_3$+drops of CD_3OD): *δ, ppm* 8.10 (d, 2H, *J* = 7.8 Hz), 7.88 (bs, 2H), 7.69 (m, 8H), 5.01 (d, 1H, *J* = 9.6 Hz), 5.00 (s, 1H), 4.28 (d, 1H, *J* = 9.6 Hz), 2.84 (s, 3H). FAB MS: *m/z* 1050 $[M]^+$ for $C_{82}H_{19}NO_2$.

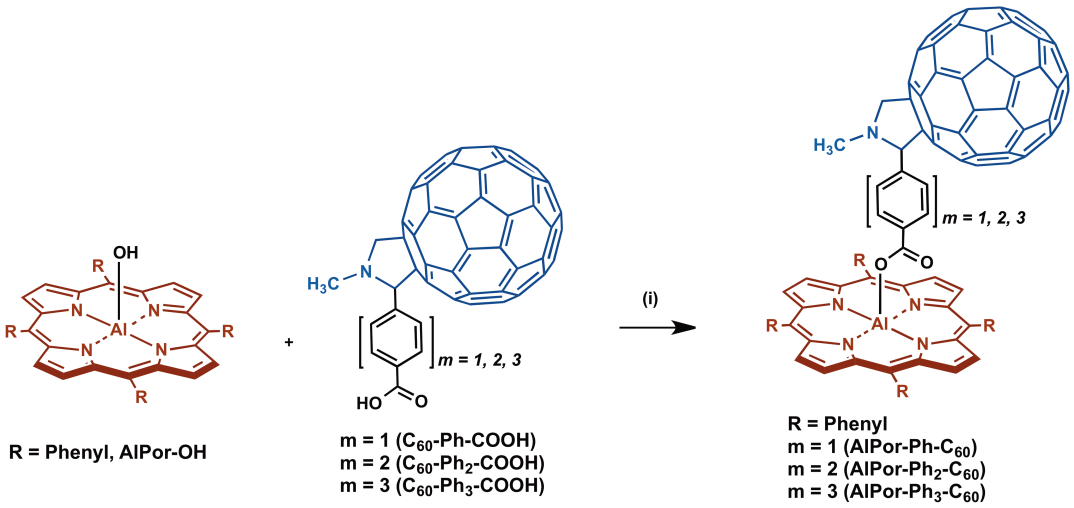

Scheme S3. Synthesis of axial aluminum(III)porphyrin-fullerene dyads. Reaction conditions: (i) Toluene, stirring at 60-80°C for 12 h under nitrogen.

Preparation of AlPor-Ph$_2$-C$_{60}$. Solution of AlPor-OH (30 mg, 0.046 mmol) and C_{60}-Ph_2-COOH (46 mg, 0.047 mmol) were dissolved in 10 ml of dry toluene, the resulting solution was stirred at 80°C for 17 h. Solvent was evaporated and washed with hexane yields the desired product in a pure form. The obtained pure compound was stored in a $CaCl_2$ desiccator. Yield: 70 mg (95%).^{1}H NMR (300 MHz, $CDCl_3$): *δ, ppm* 9.07 (s, 8H), 8.14 (d, 8H, *J* = 6.6 Hz), 7.73 (m, 16H), 6.69 (d, 2H$_b$, *J* = 8.1 Hz), 5.14 (d, 2H$_a$, *J* = 8.1 Hz), 4.93 (d, 1H, *J* = 9.3 Hz), 4.85 (s, 1H), 4.20 (d, 1H, *J* = 9.9 Hz), 2.73 (s, 3H). FAB MS: *m/z* 1611.30 $[M]^+$, Calcd. 1611.3154 for $C_{120}H_{42}AlN_5O_2$.

Preparation of AlPor-Ph$_3$-C$_{60}$. Solution of AlPor-OH (30 mg, 0.046 mmol) and C_{60}-Ph_3-COOH (49 mg, 0.047 mmol) were dissolved in 10 ml of dry toluene, the resulting solution was stirred at 80°C for 17 h. Solvent was evaporated and wash with hexane yields the desired product in pure form. The obtained pure compound was stored in a $CaCl_2$ desiccator. Yield: 74 mg (96%).^{1}H NMR (300 MHz, $CDCl_3$): *δ, ppm* 9.10 (s, 8H), 8.18 (d, 8H, *J* = 6.0 Hz), 7.77 (m, 16H), 7.63 (d, 2H, *J* = 9.0 Hz),7.54 (d, 2H, J = 9.0 Hz), 6.72 (d, 2H$_b$, *J* = 9.0 Hz), 5.21 (d, 2H$_a$, *J* = 9.0 Hz), 4.99 (d, 1H, *J* = 9.0 Hz), 4.95 (s, 1H), 4.27 (d, 1H, *J* = 9.0 Hz), 2.83 (s, 3H). FAB MS: *m/z* 1687 $[M]^+$ for $C_{126}H_{46}AlN_5O_2$.

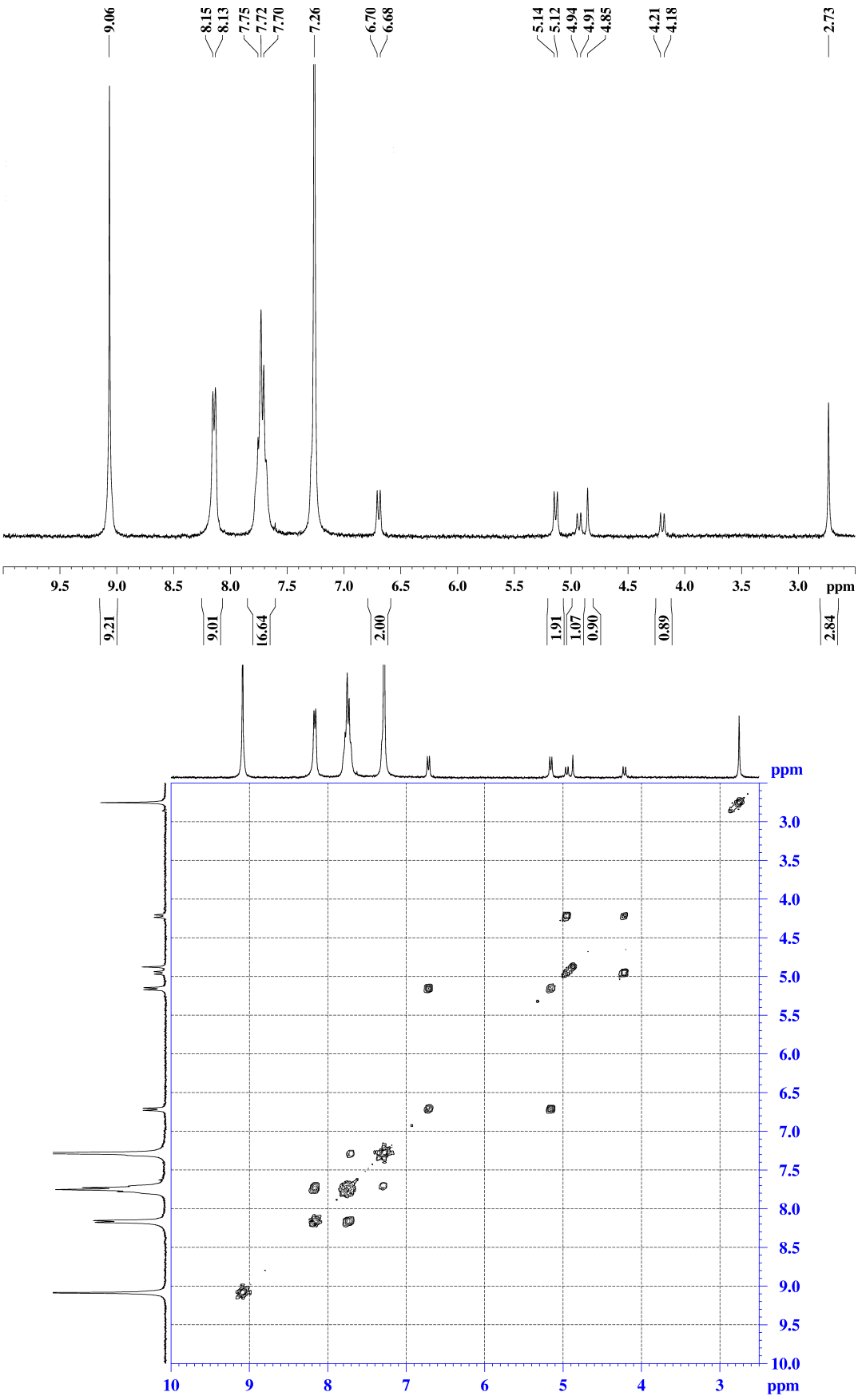

Figure S1. ^{1}H (top) and ^{1}H-^{1}H COSY (bottom) NMR spectra (300 MHz) of AlPor-Ph_2-C_{60} in $CDCl_3$.

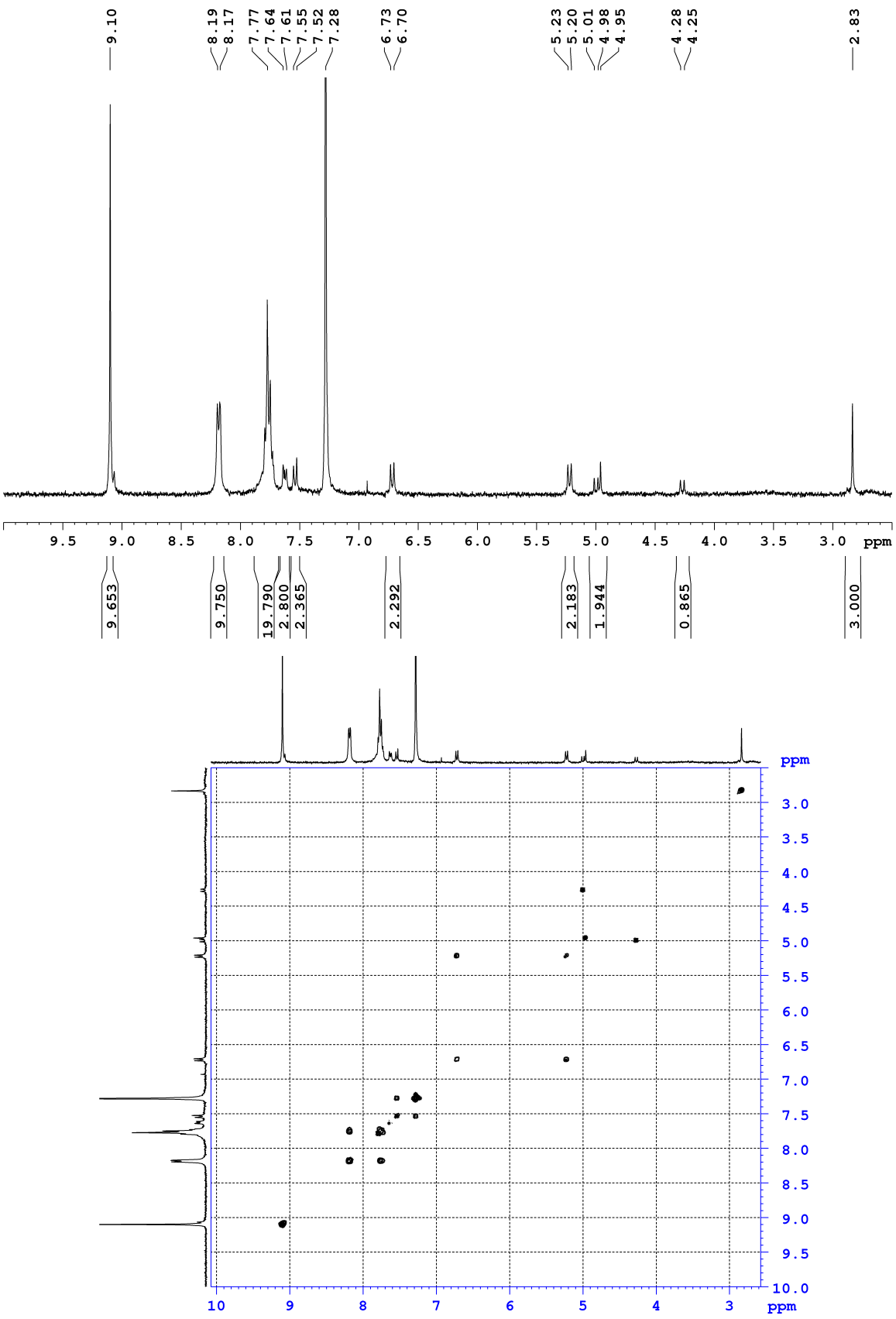

Figure S2. ^{1}H (top) and ^{1}H-^{1}H COSY (bottom) NMR spectra (300 MHz) of AlPor-Ph_3-C_{60} in $CDCl_3$.

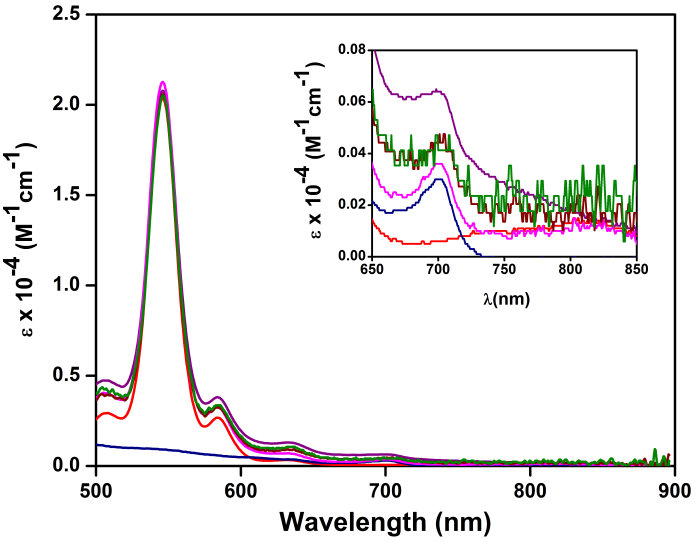

Figure S3. UV-visible absorption spectra of 0.1 mM solutions of AlPor-Ph-C_{60} (purple), AlPor-Ph_2-C_{60} (maroon), AlPor-Ph_3-C60 (green), AlPor-Ph (red), C_{60}COOMe (blue) and 1:1 mixture (magenta) of AlPor-Ph and C_{60}COOMe in dichloromethane. Inset: Magnified spectra between 650-850 nm.

Formation of supramolecular triads (TTF-Ph_n-py→AlPor-Ph_m-C_{60}). The triads shown in Scheme S4 were assembled from the components, AlPor-Ph_m-C_{60} and TTF-Ph_n-py, shown in Figure S4.

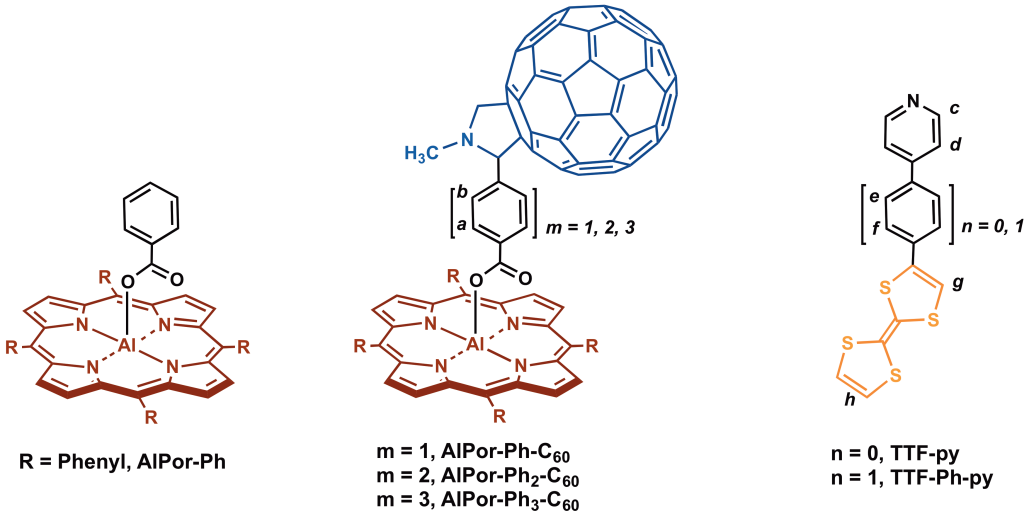

Figure S4. Structural information of investigated reference compound (AlPor-Ph), dyads and pyridine appended TTF derivatives (TTF-py and TTF-Ph-py).

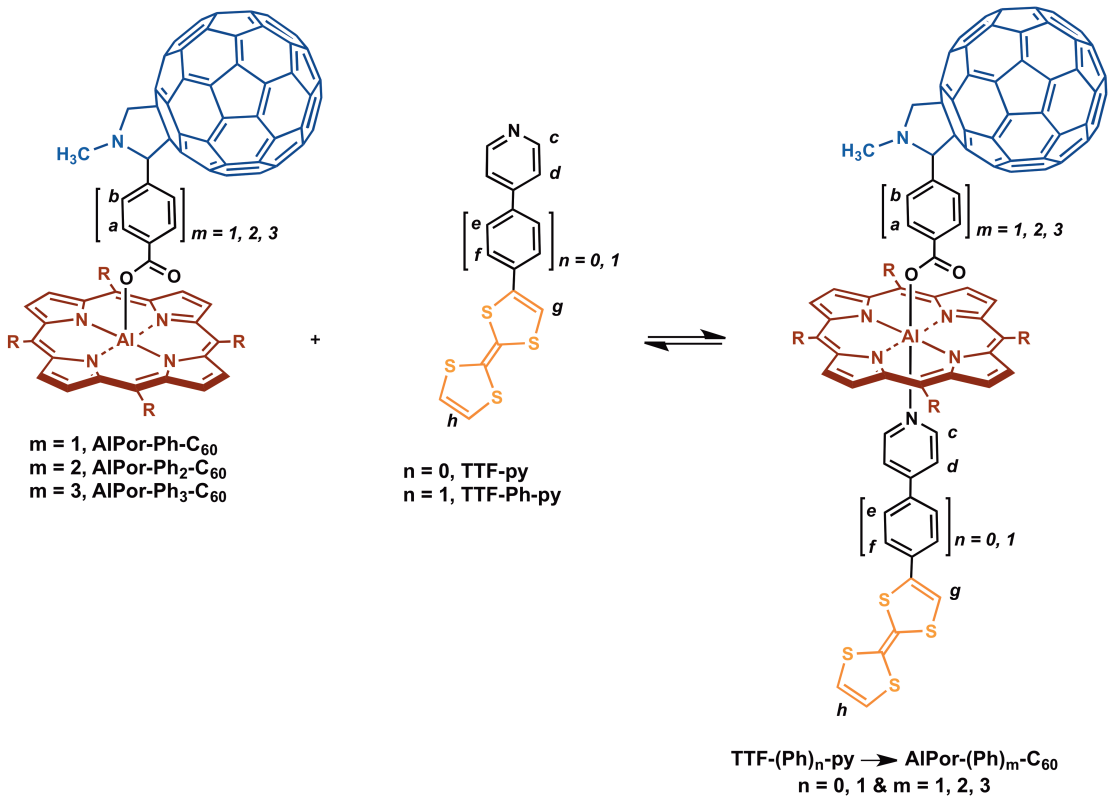

Scheme S4. Self-assembly of supramolecular TTF-Ph$_n$-py→AlPor-Ph$_m$-C$_{60}$ triads.

NMR Spectroscopy. Figure S5, shows the ^{1}H NMR spectrum of a 1:1 mixture of AlPor-Ph-C$_{60}$ and TTF-Ph-py (top) along with the individual spectra of AlPor-Ph-C$_{60}$ (middle) and TTF-Ph-py (bottom). In the coordination complex, shielding due to the porphyrin ring causes an upfield shift of the TTF-Ph-py protons on the pyridine unit (*c* and *d*) as well as bridging phenyl moiety (e and *f*). The magnitude of the shift depends on the distance of the protons from the porphyrin ring and the pyridinyl protons (*c* and *d*) display the greatest shift indicating that coordination occurs via the pyridinyl group. Small shift was observed for TTF protons *g* and *h* suggests TTF unit is away from porphyrin ring. On the benzoate bridging group to the fullerene, the protons (*a*) closest to the porphyrin ring show an increased upfield shift upon coordination, suggesting that the Al center lies out of the porphyrin plane in AlPor-Ph-C$_{60}$ and is pulled into the plane when TTF-Ph-py coordinates. Similar ^{1}H NMR titrations were carried out for the triad TTF-py→AlPor-Ph-C$_{60}$ and the results show shielding effects for the py and TTF protons, Figure S6. Overall, the NMR titrations confirm the formation of triads the TTF-py→AlPor-Ph-C$_{60}$ and TTF-Ph-py→AlPor-Ph-C$_{60}$.

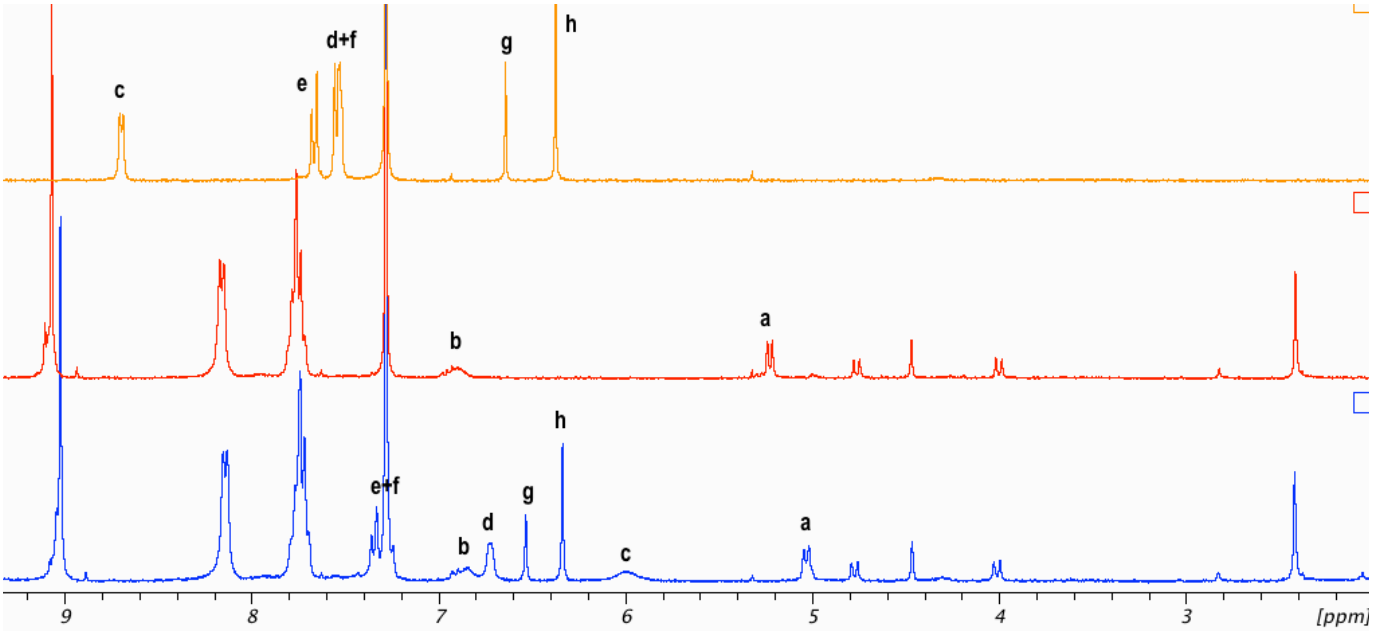

Figure S5. ^{1}H NMR (300 MHz) spectra of 2.3 mM solutions of TTF-Ph-py (bottom), AlPor-Ph-C_{60} (middle) and TTF-Ph-py→AlPor-Ph-C_{60} (top) in $CDCl_3$.

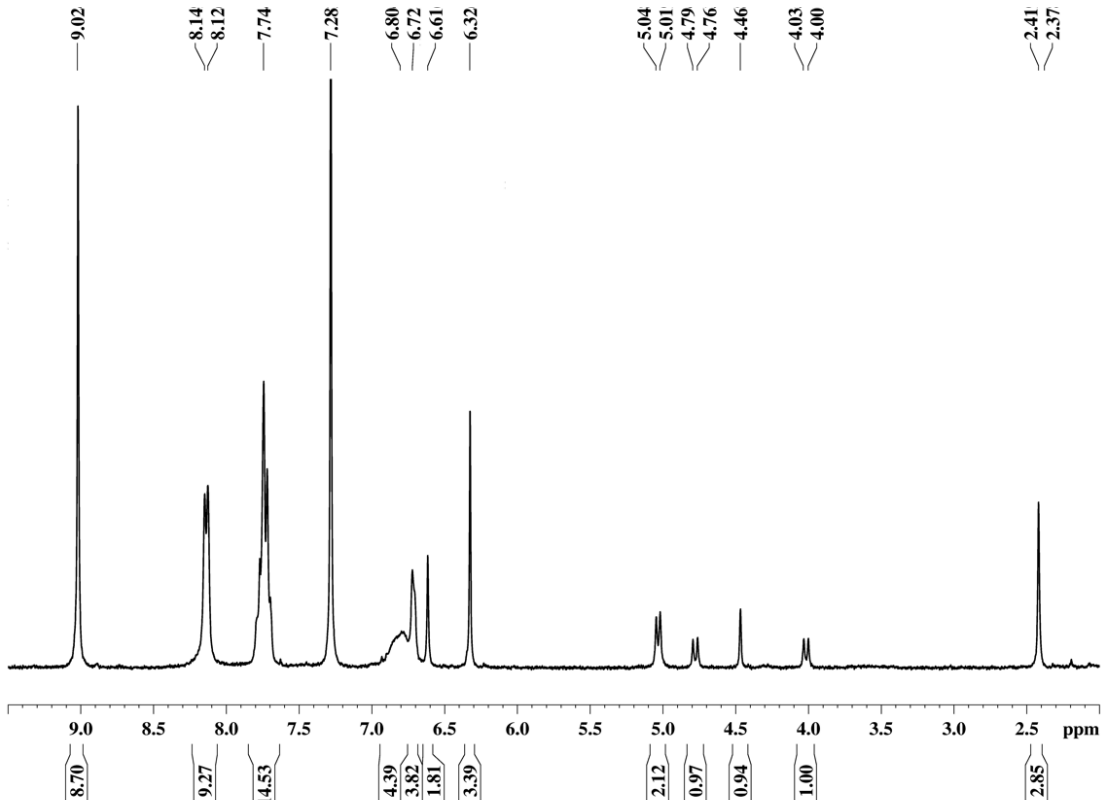

Figure S6. ^{1}H NMR spectrum (300 MHz) of 2.9 mM TTF-py→AlPor-Ph-C_{60} in $CDCl_3$.

Table S1. Optical and electrochemistry data of the triads, dyads and their reference compounds.

Sample	Binding Constant (M^{-1})	Absorption[a] λ_{max}, nm (log ε)		Potential (V) *vs* Fc[b]	
		TTF/C_{60}/B-Bands	Q-Bands	Oxidation	Reduction
AlPor-Ph-C_{60}	-	256 (5.06), 307 (4.68), 416 (5.72)	547 (4.33), 585 (3.52)	1.10	–0.44, –0.83, –1.00, –1.39
TTF-py→AlPor-Ph-C_{60}	1248	-	-	0.68, 1.02, 1.11	–0.44, –0.82, –1.00, –1.39
TTF-Ph-py→AlPor-Ph-C_{60}	1217	-	-	0.71, 1.07	–0.42, –0.82, –1.00, –1.37
py→AlPor-Ph-C_{60}	1307	-	-	-	-
AlPor-Ph_2-C_{60}	-	256 (5.07), 307 (4.76), 415 (5.74)	546 (4.32), 583 (3.51)	1.10	–0.42, –0.77, –1.04, –1.37
TTF-py→AlPor-Ph_2-C_{60}	1325	-	-	-	-
TTF-Ph-py→AlPor-Ph_2-C_{60}	1544	-	-	-	-
py→AlPor-Ph_2-C_{60}	1352	-	-	-	-
AlPor-Ph_3-C_{60}	-	257 (5.09), 307 (4.93), 415 (5.74)	546 (4.32), 584 (3.53)	1.14	–0.39, –0.75, –1.05, –1.31
TTF-py→AlPor-Ph_3-C_{60}	1337	-	-	-	-
TTF-Ph-py→AlPor-Ph_3-C_{60}	1352	-	-	-	-
py→AlPor-Ph_3-C_{60}	1450	-	-	-	-
AlPor-Ph	-	415 (5.75)	546 (4.34), 585 (3.43)	1.12	–0.97, –1.35
TTF-py→AlPor-Ph	1075	-	-	0.68, 1.01, 1.14	–1.00, –1.35
TTF-Ph-py→AlPor-Ph	1047	-	-	0.72, 1.05	–0.94, –1.30
py→AlPor-Ph	1170	-	-	-	-
C_{60}-Ph-COOMe	-	256 (5.06), 309 (4.55)	-	-	–0.40, –0.78, –1.31
TTF-py	-	285 (4.22), 324 (4.17), 435 (3.45)	-	0.69, 1.00	-
TTF-Ph-py	-	298 (4.48), 428 (3.64)	-	0.73, 1.10	-

[a]In dichloromethane. [b]Redox potentials were reported against ferrocene, where $E_{1/2}(Fc/Fc^{+})$ = 0.74 V with 0.1 M TBAP in *o*-DCB in our experimental conditions.

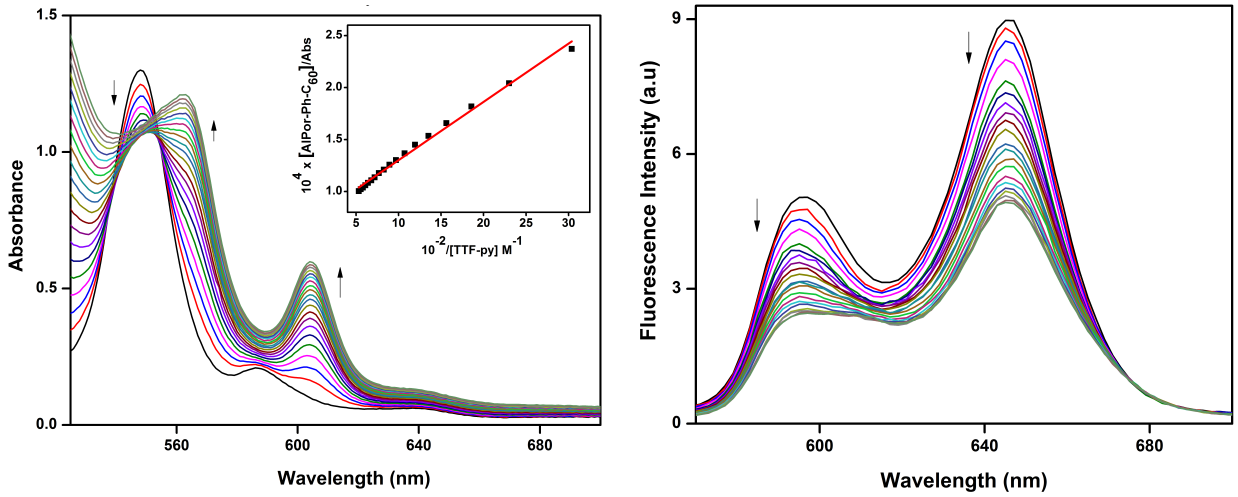

Figure S7. Spectral titrations of AlPor-Ph-C_{60} with TTF-py in *o*-DCB. TTF-py was added up to 1.9×10^{-3} M in 1.12×10^{-4} M increments to a 6×10^{-5} M solution of AlPor-Ph-C_{60}. Left: Absorption titrations, inset shows the Benesi-Hildebrand plot of the change of absorbance at 604 nm. Right: Fluorescence titrations, the excitation wavelength was chosen at the isosbestic point, 555 nm, obtained from UV-visible titrations.

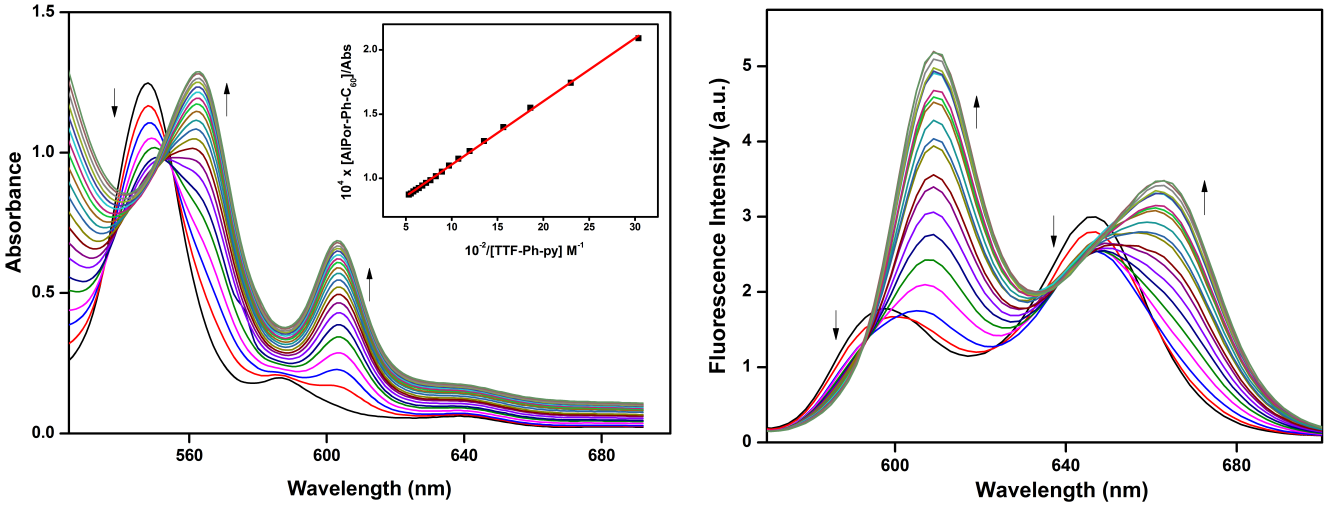

Figure S8. Spectral titration of AlPor-Ph-C_{60} with TTF-Ph-py in *o*-DCB. TTF-Ph-py was added up to 1.9×10^{-3} M in 1.12×10^{-4} M increments to a 6×10^{-5} M solution of AlPor-Ph-C_{60}. Left: Absorption titrations, inset shows the Benesi-Hildebrand plot of the change of absorbance at 604 nm. Right: Fluorescence titrations, the excitation wavelength was chosen at the isosbestic point, 555 nm, obtained from UV-visible titrations.

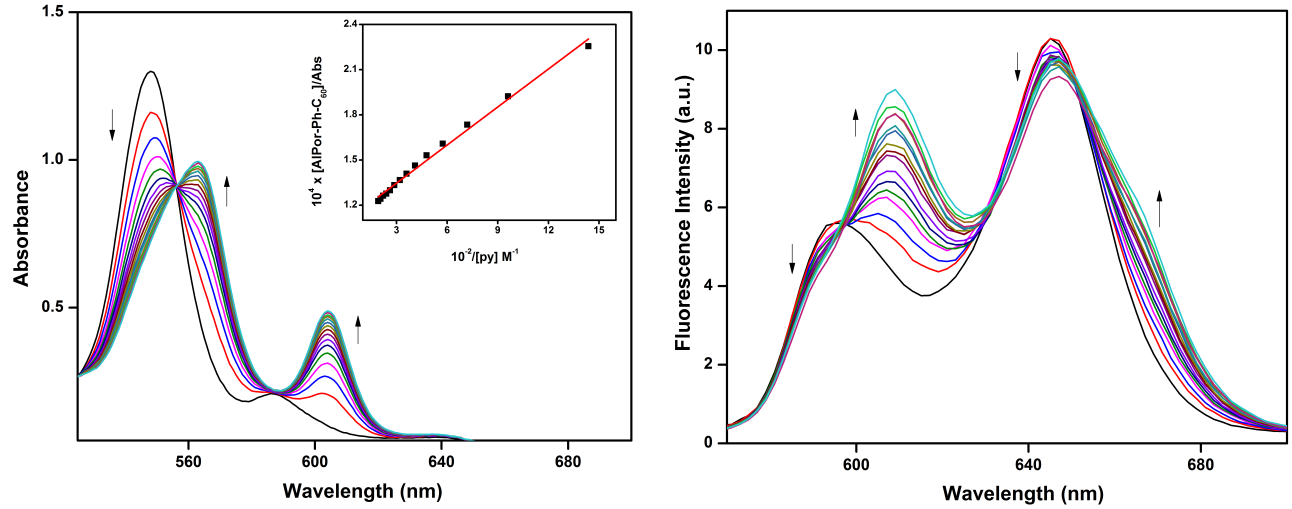

Figure S9. Spectral titrations of AlPor-Ph-C_{60} with py in *o*-DCB. Pyridine was added up to 4.51×10^{-3} M in 3.48×10^{-4} M increments to a 6×10^{-5} M solution of AlPor-Ph-C_{60}. Left: Absorption titrations, inset shows the Benesi-Hildebrand plot of the change of absorbance at 604 nm. Right: Fluorescence titrations, the excitation wavelength was chosen at the isosbestic point, 555 nm, obtained from UV-visible titrations.

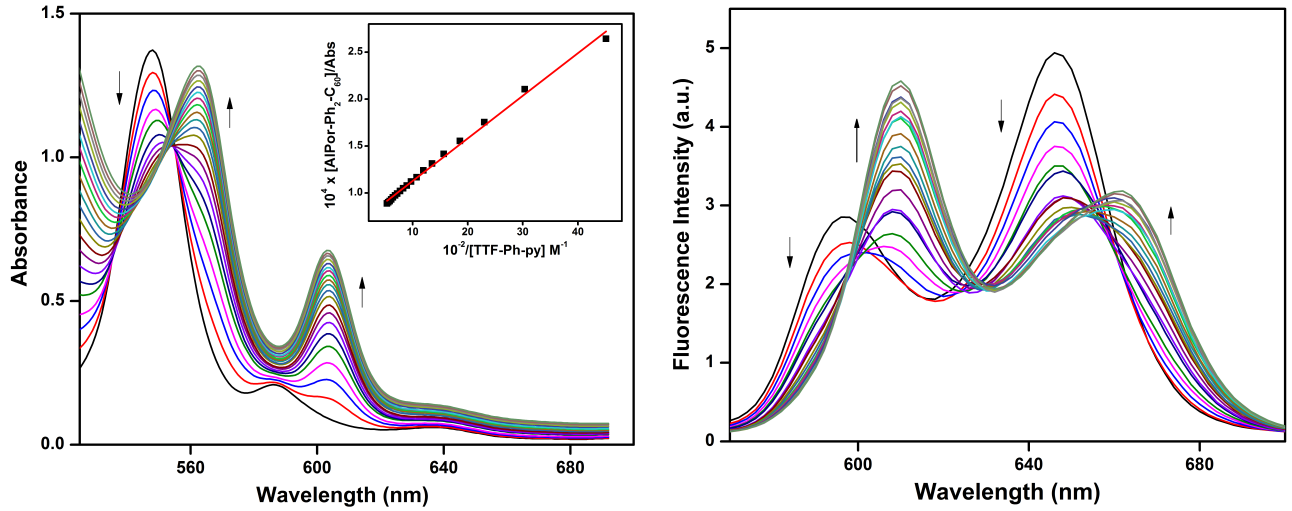

Figure S10. Spectral titrations of AlPor-Ph_2-C_{60} with TTF-Ph-py in *o*-DCB. TTF-Ph-py was added up to 1.9×10^{-3} M in 1.12×10^{-4} M increments to a 6×10^{-5} M solution of AlPor-Ph_2-C_{60}. Left: Absorption titrations, inset shows the Benesi-Hildebrand plot of the change of absorbance at 604 nm. Right: Fluorescence titrations, the excitation wavelength was chosen at the isosbestic point, 554 nm, obtained from UV-visible titrations.

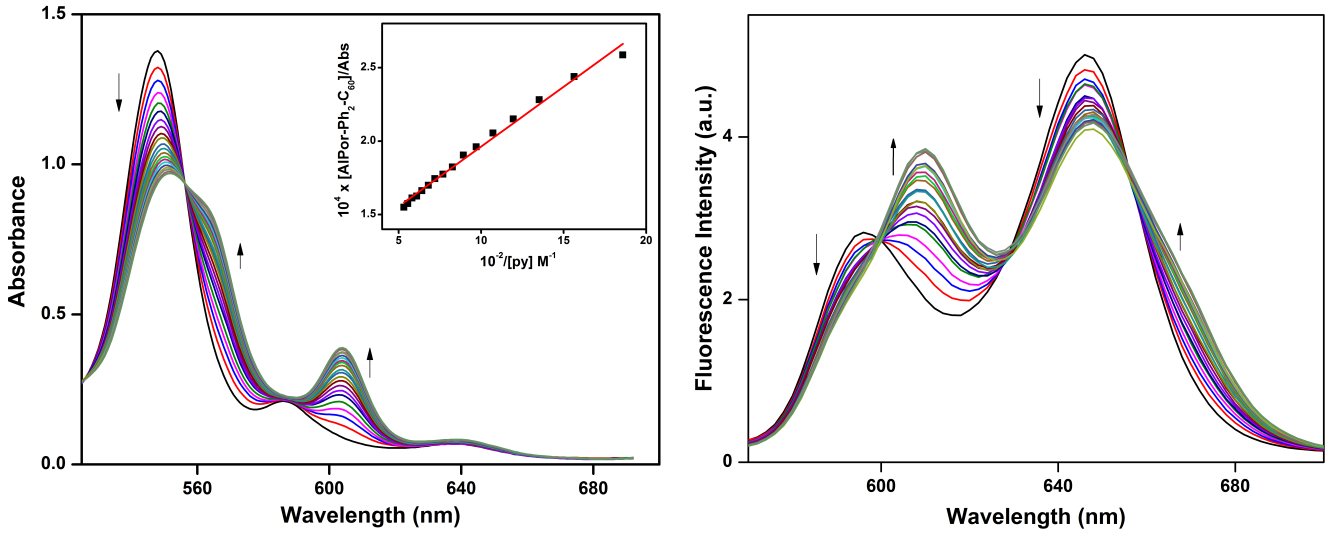

Figure S11. Spectral titrations of AlPor-Ph_2-C_{60} with py in *o*-DCB. Pyridine was added up to 1.9×10^{-3} M in 1.12×10^{-4} M increments to a 6×10^{-5} M solution of AlPor-Ph_2-C_{60}. Left: Absorption titrations, inset shows the Benesi-Hildebrand plot of the change of absorbance at 604 nm. Right: Fluorescence titrations, the excitation wavelength was chosen at the isosbestic point, 555 nm, obtained from UV-visible titrations.

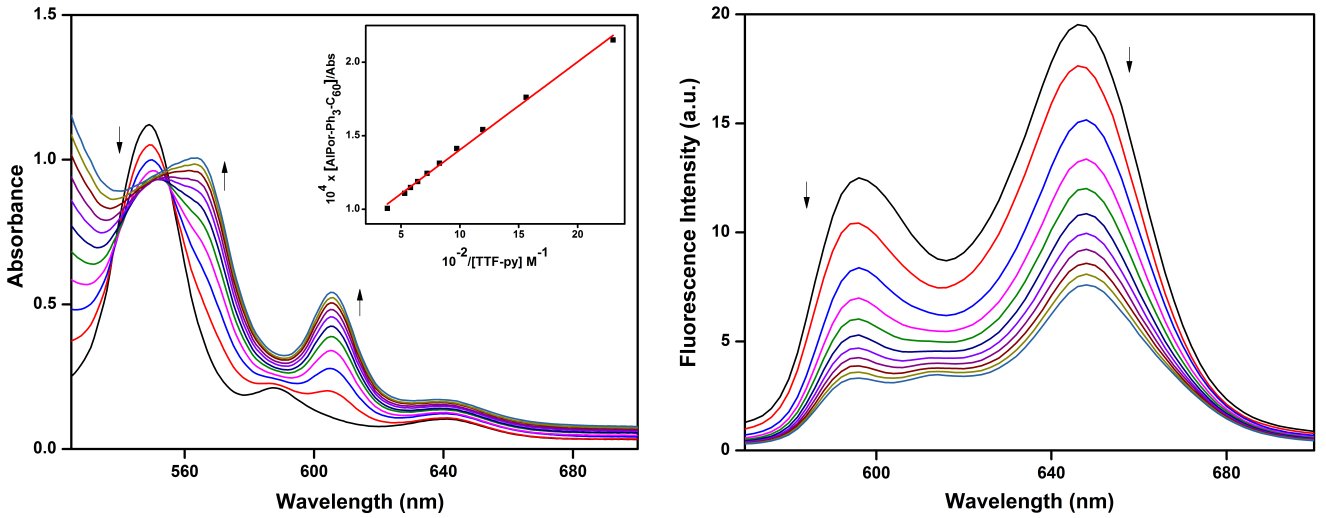

Figure S12. Spectral titrations of AlPor-Ph_3-C_{60} with TTF-py in *o*-DCB. TTF-py was added up to 1.9×10^{-3} M in 1.12×10^{-4} M increments to a 6×10^{-5} M solution of AlPor-Ph_3-C_{60}. Left: Absorption titrations, inset shows the Benesi-Hildebrand plot of the change of absorbance at 604 nm. Right: Fluorescence titrations, the excitation wavelength was chosen at the isosbestic point, 555 nm, obtained from UV-visible titrations.

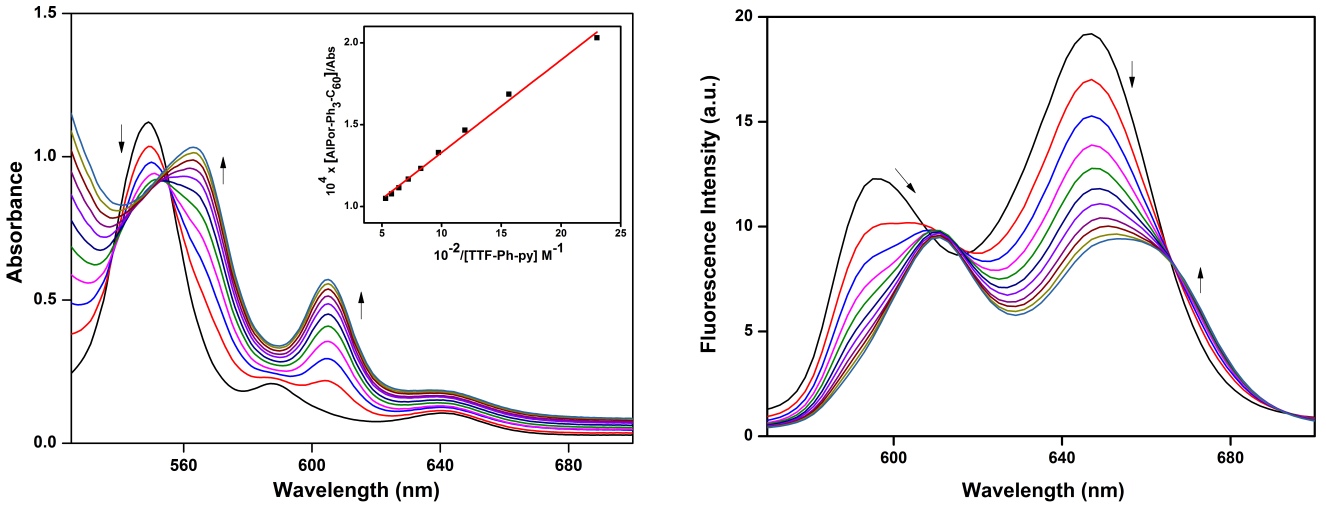

Figure S13. Spectral titrations of AlPor-Ph_3-C_{60} with TTF-Ph-py in *o*-DCB. TTF-Ph-py was added up to 1.9×10^{-3} M in 1.12×10^{-4} M increments to a 6×10^{-5} M solution of AlPor-Ph_3-C_{60}. Left: Absorption titrations, inset shows the Benesi-Hildebrand plot of the change of absorbance at 605 nm. Right: Fluorescence titrations, the excitation wavelength was chosen at the isosbestic point, 555 nm, obtained from UV-visible titrations.

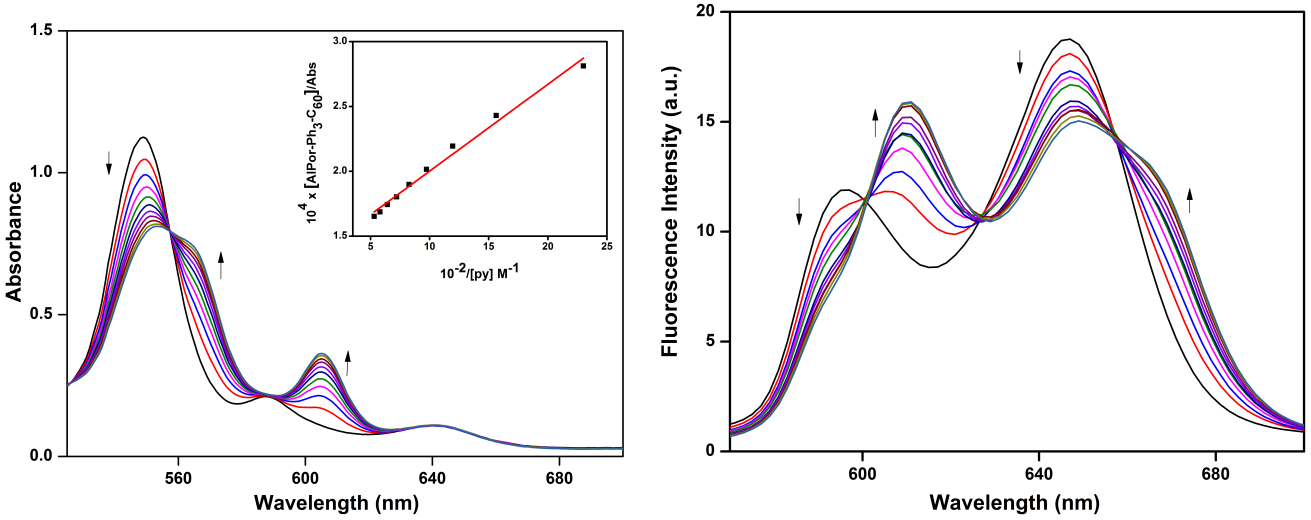

Figure S14. Spectral titrations of AlPor-Ph_3-C_{60} with py in *o*-DCB. Pyridine was added up to 1.9×10^{-3} M in 1.12×10^{-4} M increments to a 6×10^{-5} M solution of AlPor-Ph_3-C_{60}. Left: Absorption titrations, inset shows the Benesi-Hildebrand plot of the change of absorbance at 605 nm. Right: Fluorescence titrations, the excitation wavelength was chosen at the isosbestic point, 555 nm, obtained from UV-visible titrations.

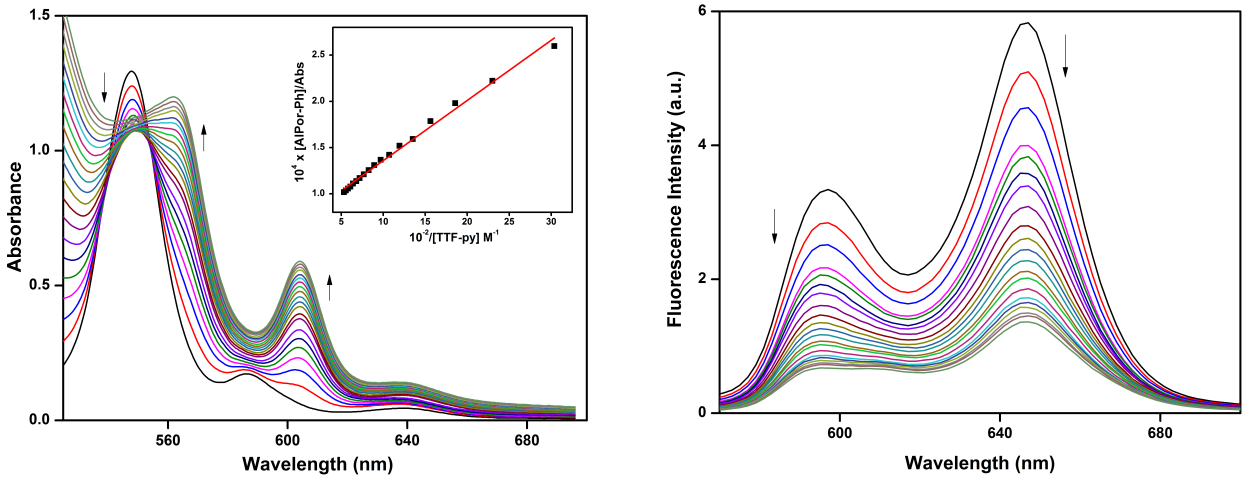

Figure S15. Spectral titrations of AlPor-Ph with TTF-py in *o*-DCB. TTF-py was added up to 1.9×10^{-3} M in 1.12×10^{-4} M increments to a 6×10^{-5} M solution of AlPor-Ph. Left: Absorption titrations, inset shows the Benesi-Hildebrand plot of the change of absorbance at 604 nm. Right: Fluorescence titrations, the excitation wavelength was chosen at the isosbestic point, 555 nm, obtained from UV-visible titrations.

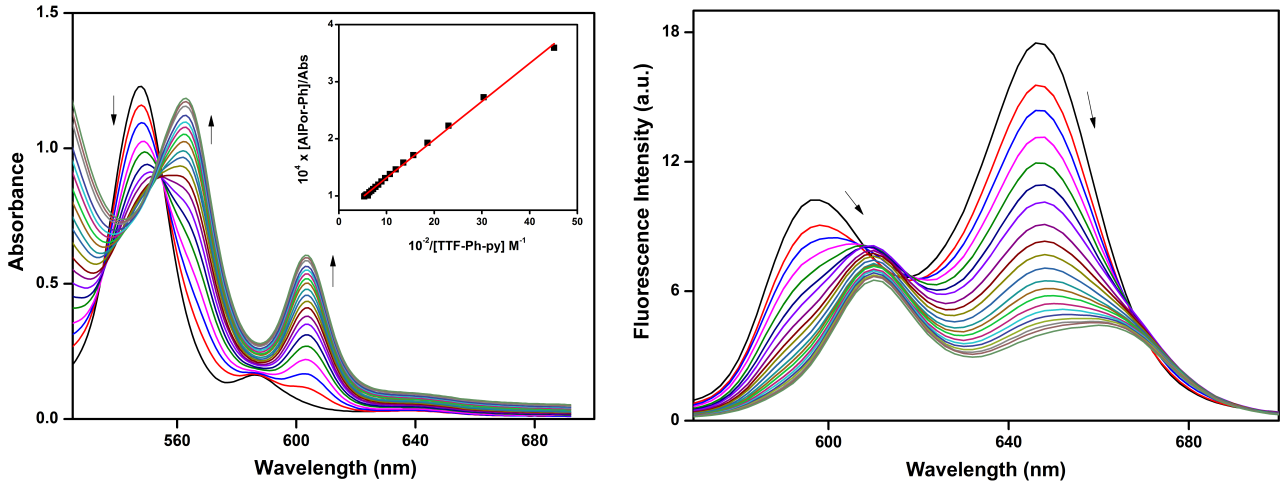

Figure S16. Spectral titrations of AlPor-Ph with TTF-Ph-py in *o*-DCB. TTF-Ph-py was added up to 1.9 × 10^{-3} M in 1.12 × 10^{-4} M increments to a 6 × 10^{-5} M solution of AlPor-Ph. Left: Absorption titrations, inset shows the Benesi-Hildebrand plot of the change of absorbance at 604 nm. Right: Fluorescence titrations, the excitation wavelength was chosen at the isosbestic point, 554 nm, obtained from UV-visible titrations.

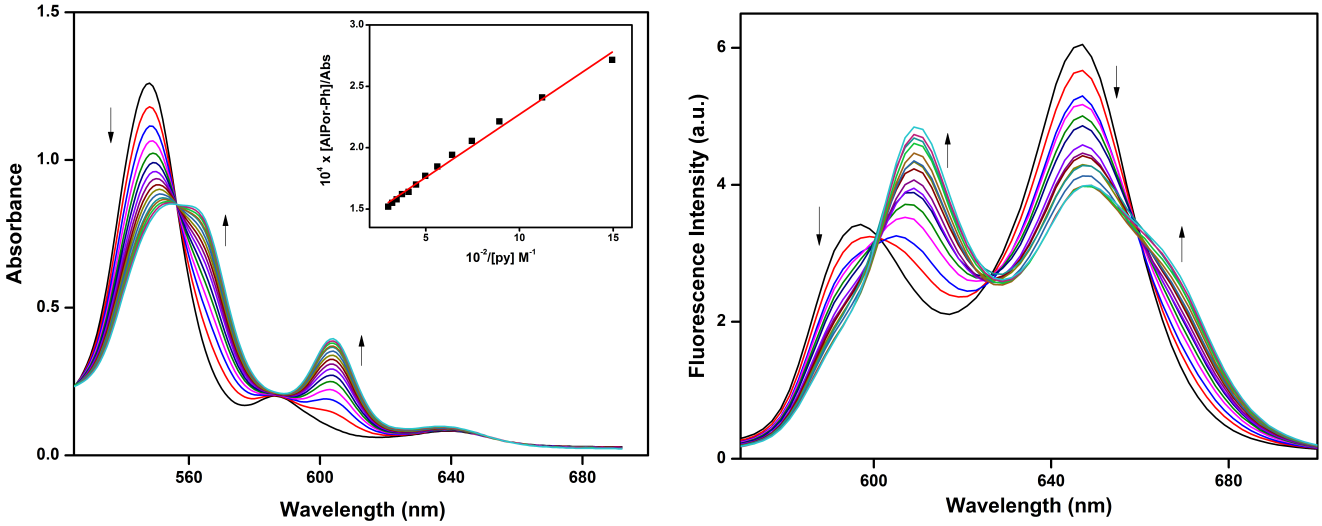

Figure S17. Spectral titrations of AlPor-Ph with py in *o*-DCB. Pyridine was added up to 4.5 × 10^{-3} M in 2.23 × 10^{-4} M increments to a 6 × 10^{-5} M solution of AlPor-Ph. Left: Absorption titrations, inset shows the Benesi-Hildebrand plot of the change of absorbance at 604 nm. Right: Fluorescence titrations, the excitation wavelength was chosen at the isosbestic point, 555 nm, obtained from UV-visible titrations.

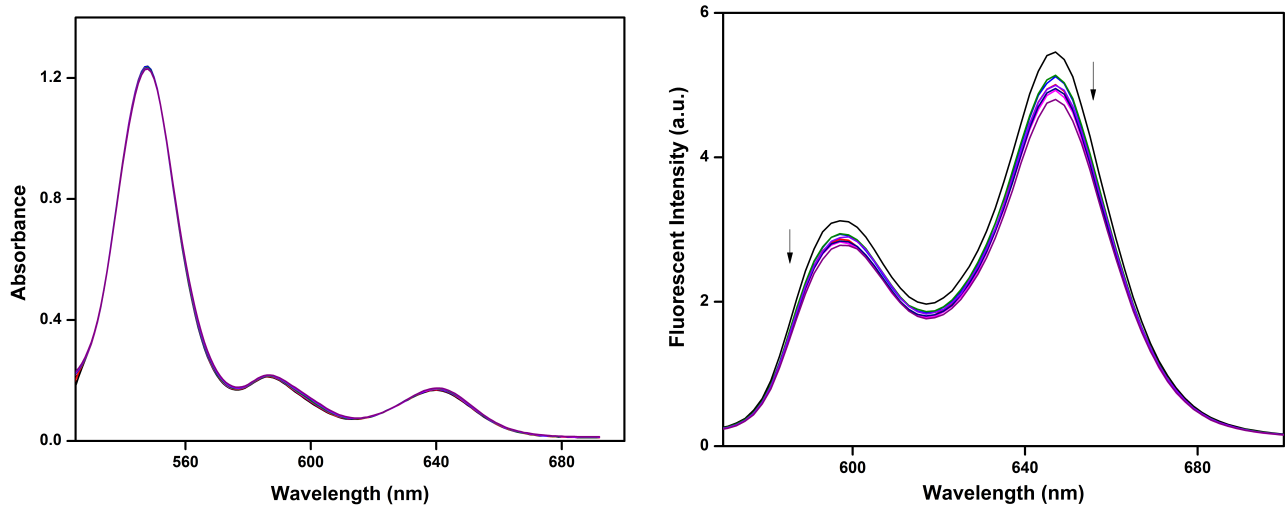

Figure S18. Spectral titrations of AlPor-Ph with TTF in *o*-DCB. TTF was added up to 3.53×10^{-3} M in 2.10×10^{-4} M increments to solution of 6×10^{-5} M solution of AlPor-Ph. Left: Absorption titrations. Right: Fluorescence titrations, the excitation wavelength was chosen to be 555 nm.

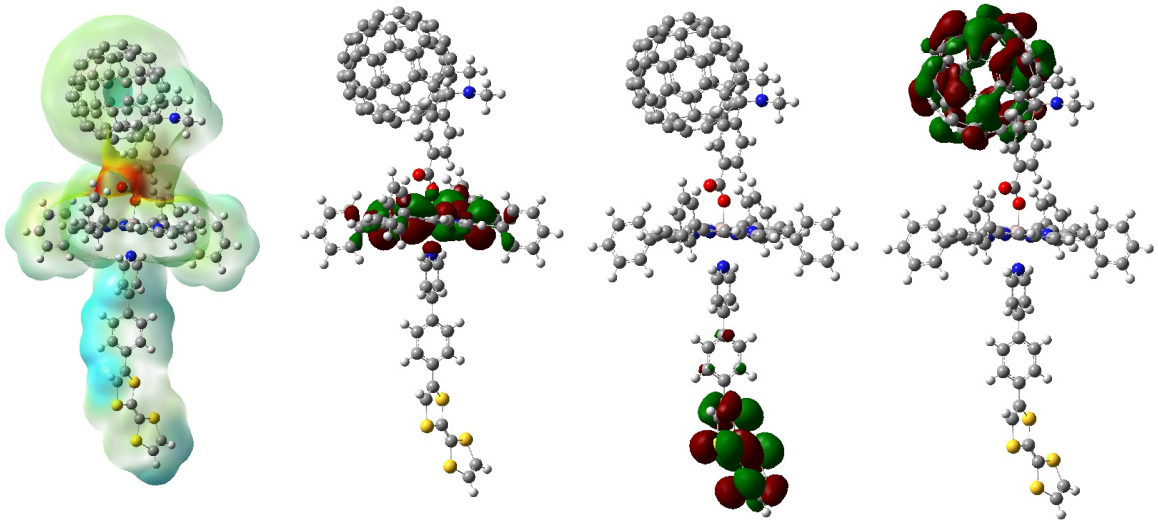

Figure S19. Molecular electrostatic potential map (MEP), HOMO-1, HOMO and LUMO of TTF-Ph-py→AlPor-*Ph*-C_{60}.

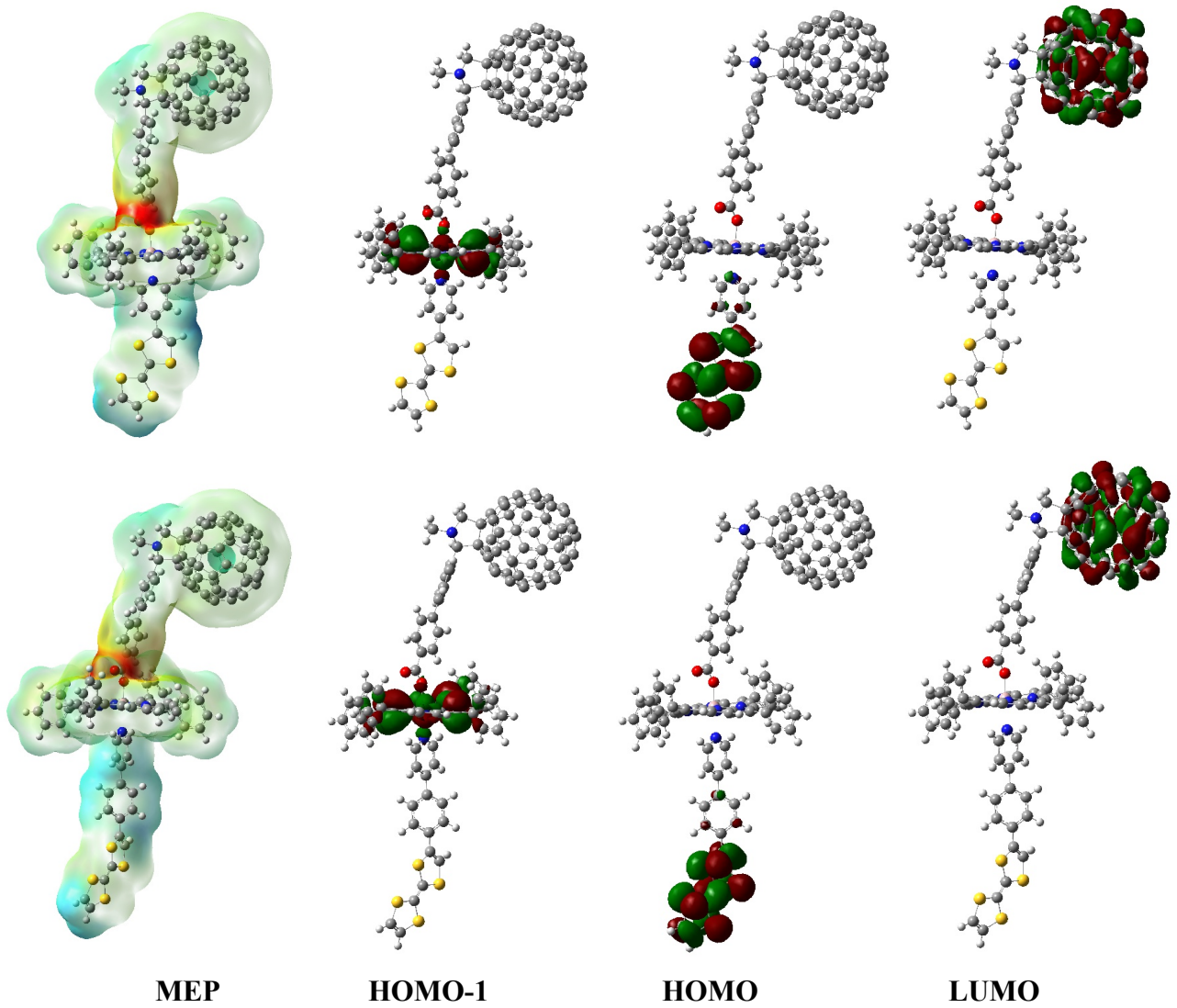

Figure S20. Molecular electrostatic potential map (MEP), HOMO-1, HOMO and LUMO of TTF-py→AlPor-*Ph*$_2$-C$_{60}$ (top) and TTF-*Ph*-py→AlPor-*Ph*$_2$-C$_{60}$ (bottom).

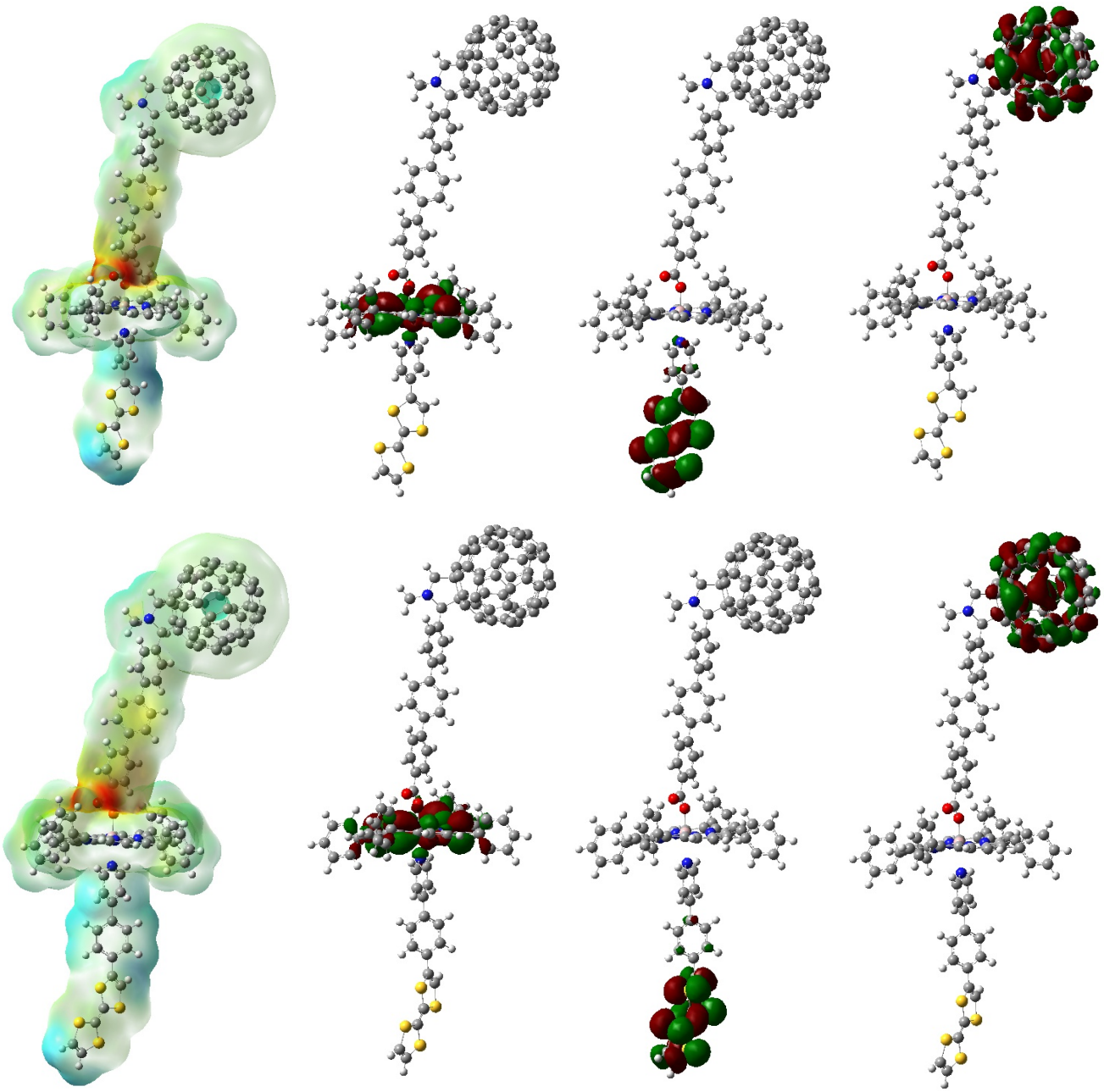

MEP **HOMO-1** **HOMO** **LUMO**

Figure S21. Molecular electrostatic potential map (MEP), HOMO-1, HOMO and LUMO of TTF-py→AlPor-*Ph*$_3$-C$_{60}$ (top) and TTF-*Ph*-py→AlPor-*Ph*$_3$-C$_{60}$ (bottom).

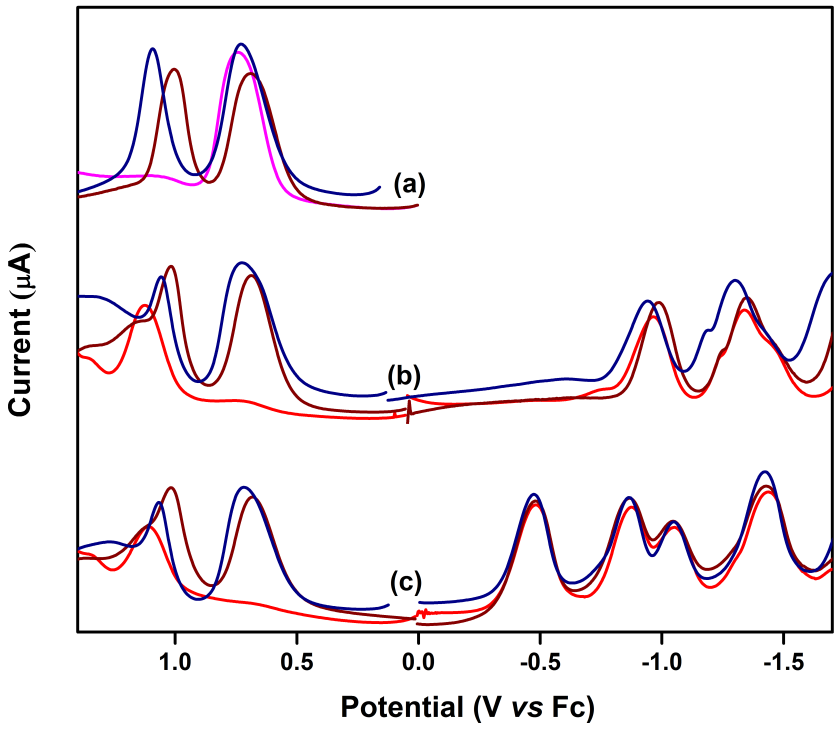

Figure S22. Differential pulse voltammograms of (a) Ferrocene (magenta), TTF-py (maroon) and TTF-Ph-py (blue) (b) 0.52 mM solution of AlPor-Ph (red), TTF-py→AlPor-Ph (maroon) and TTF-Ph-py→AlPor-Ph (blue) (c) 0.43 mM solution of AlPor-Ph-C_{60} (red), TTF-py→AlPor-Ph-C_{60} (maroon) and TTF-Ph-py→AlPor-Ph-C_{60} (blue) in 0.1 M TBAP, *o*-DCB.

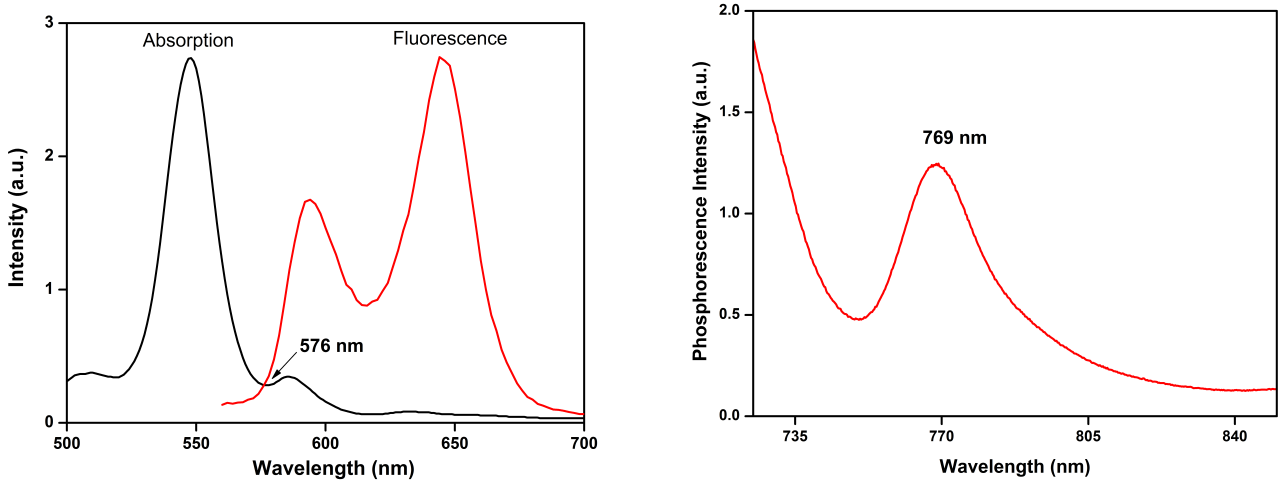

Figure S23. Left: Absorption (black) and fluorescence (red) spectra of AlPor-Ph in *o*-DCB at room temperature. Right: Phosphorescence spectrum of AlPor-Ph in CH_2Cl_2:C_2H_5OH (= 1:1) at 77K.

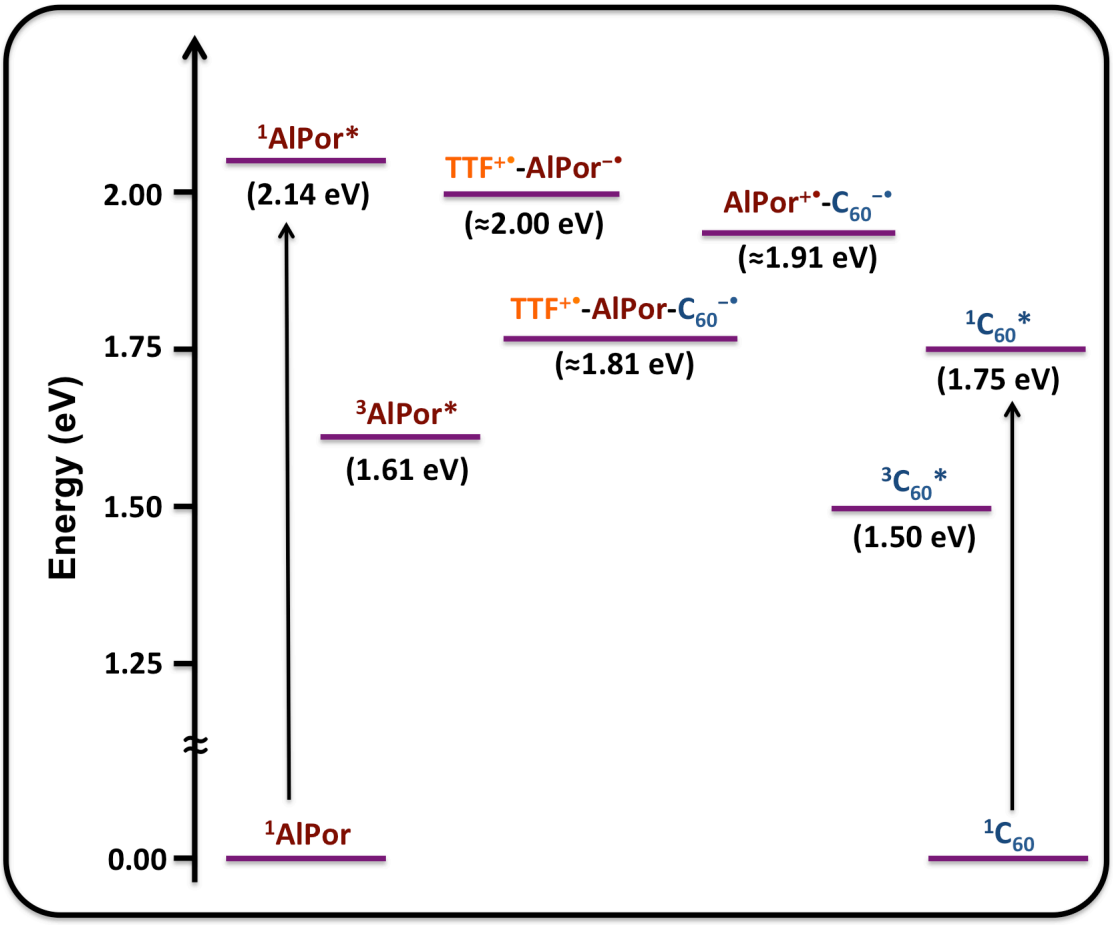

Figure S24. Diagram illustrating the energies of the possible charge separated states in newly constructed dyads and triads in toluene. Note that the reported energies for $TTF^{+\bullet}AlPor^{-\bullet}$, $AlPor^{+\bullet}C_{60}^{-\bullet}$ and $TTF^{+\bullet}C_{60}^{-\bullet}$ are average values of two dyads (TTF-Ph_n-py→AlPor-Ph, n = 0, 1), three dyads (AlPor-Ph_m-C_{60}, m = 1-3) and six triads (TTF-Ph_n-py→AlPor-Ph_m-C_{60}, n = 0, 1 & m = 1-3), respectively.

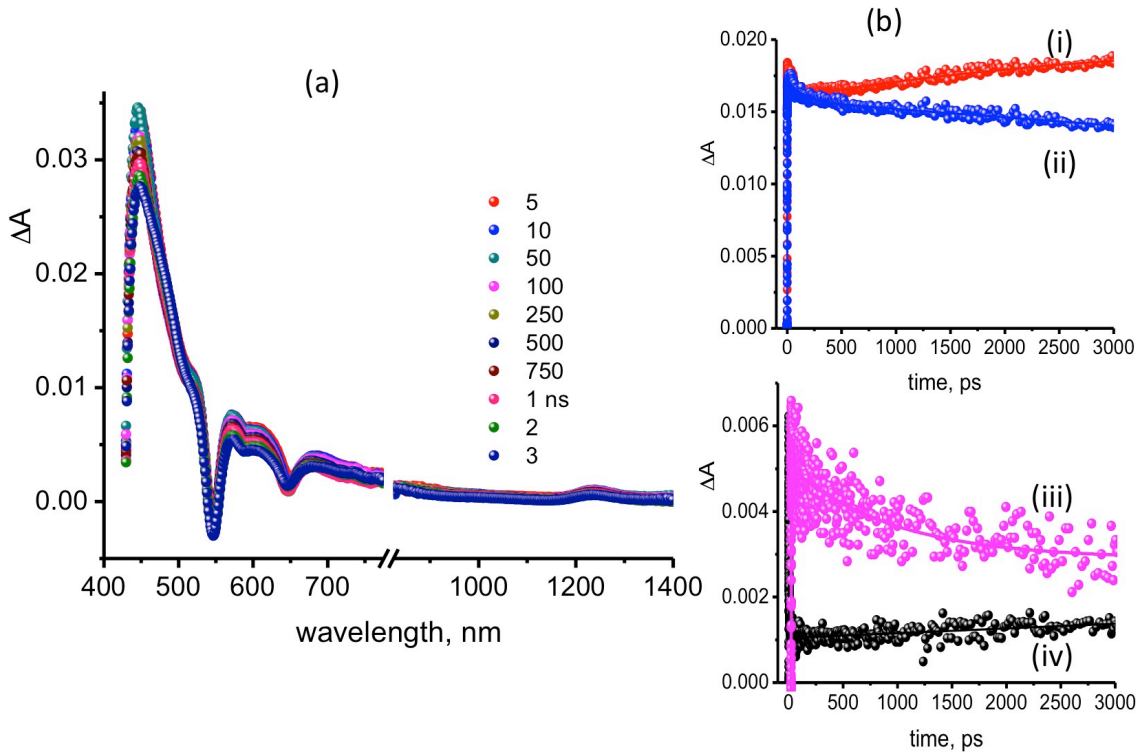

Figure S25. Femtosecond transient spectra of AlPor-Ph in toluene at the indicated time intervals. The time profiles of (i) 487, (ii) 448, (iii) 1240 and (iv) 648 nm are shown.

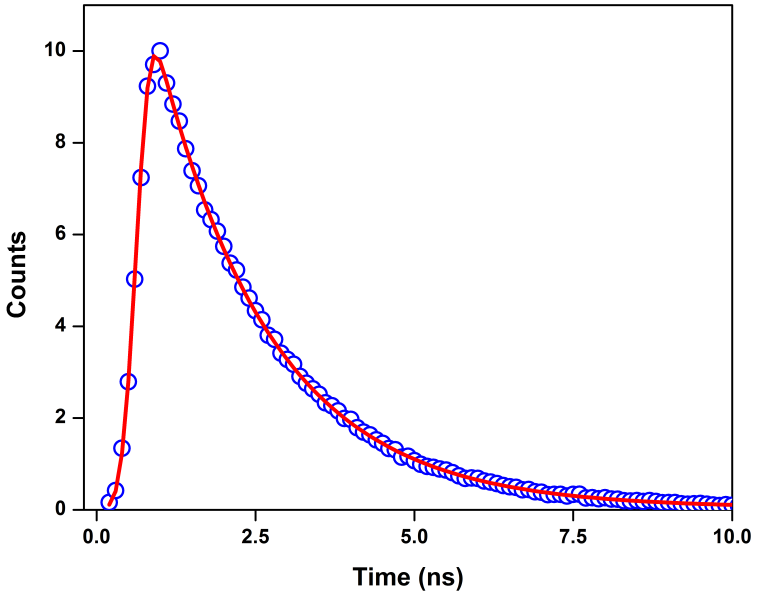

Figure S26. Fluorescence decay curve of AlPor-Ph in Ar-saturated toluene. Excitation and emission wavelengths were at 560 and 590 nm, respectively.

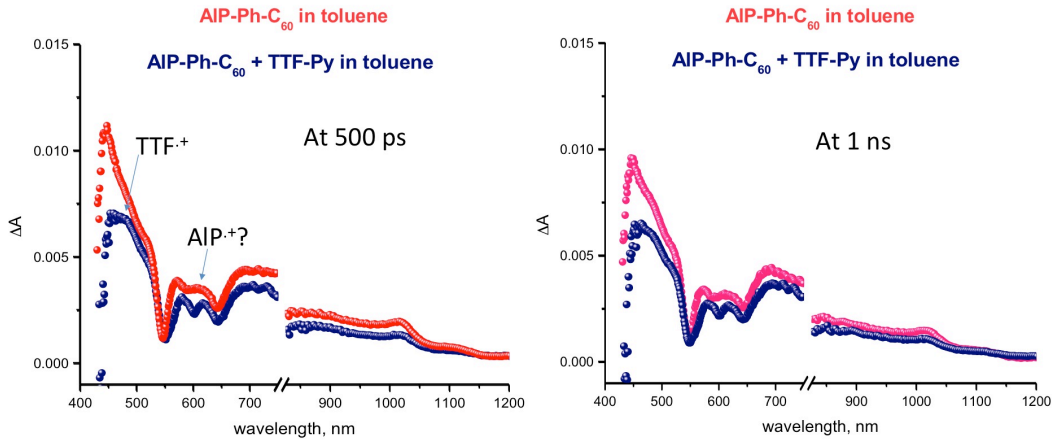

Figure S27. Femtosecond transient absorption spectra of AlPor-Ph-C_{60} and TTF-py→AlPor-Ph-C_{60} ls in toluene at different time intervals.

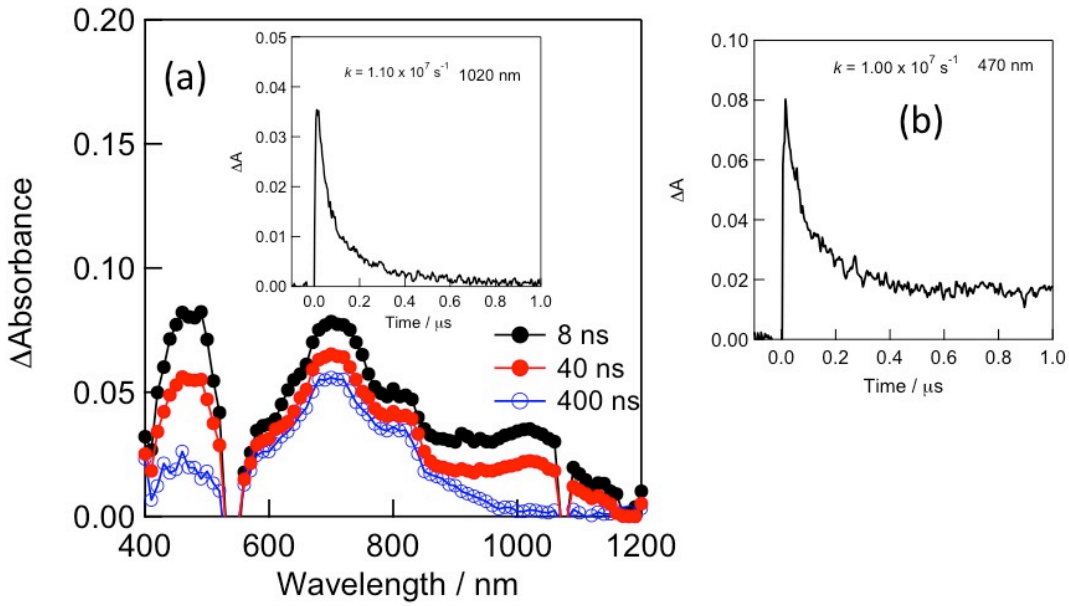

Figure S28. (a) Nanosecond transient absorption spectra of 0.1 mM TTF-Ph-py→AlPor-Ph-C_{60} observed by 532 nm (ca. 3 mJ/pulse) laser irradiation in *o*-DCB. Inset: Absorption-time profile at 1020 nm. (b) Absorption time profile at 470 nm.

References

(1) Poddutoori, P. K.; Sandanayaka, A. S. D.; Hasobe, T.; Ito, O.; van der Est, A. *J Phys Chem B* **2010**, *114*, 14348.

(2) Poddutoori, P. K.; Sandanayaka, A. S. D.; Zarrabi, N.; Hasobe, T.; Ito, O.; van der Est, A. *J Phys Chem A* **2011**, *115*, 709.

(3) Poddutoori, P. K.; Zarrabi, N.; Moiseev, A. G.; Gumbau-Brisa, R.; Vassiliev, S.; van der Est, A. *Chem. Eur. J.* **2013**, *19*, 3148.

(4) Fujimori, T.; Wirsching, P.; Janda, K. D. *J Comb Chem* **2003**, *5*, 625.

(5) Miyaura, N.; Suzuki, A. *Chem Rev* **1995**, *95*, 2457.

(6) Simoni, D.; Giannini, G.; Roberti, M.; Rondanin, R.; Baruchello, R.; Rossi, M.; Grisolia, G.; Invidiata, F. P.; Aiello, S.; Marino, S.; Cavallini, S.; Siniscalchi, A.; Gebbia, N.; Crosta, L.; Grimaudo, S.; Abbadessa, V.; Di Cristina, A.; Tolomeo, M. *J Med Chem* **2005**, *48*, 4293.